

Localized Iron Supply Triggers Lateral Root Elongation in *Arabidopsis* by Altering the AUX1-Mediated Auxin Distribution

Ricardo F.H. Giehl,^{a,b,1} Joni E. Lima,^{a,1,2} and Nicolaus von Wirén^{a,b,3}

^a Molecular Plant Nutrition, University of Hohenheim, D-70593 Stuttgart, Germany

^b Leibniz-Institute for Plant Genetics and Crop Plant Research, D-06466 Gatersleben, Germany

Root system architecture depends on nutrient availability, which shapes primary and lateral root development in a nutrient-specific manner. To better understand how nutrient signals are integrated into root developmental programs, we investigated the morphological response of *Arabidopsis thaliana* roots to iron (Fe). Relative to a homogeneous supply, localized Fe supply in horizontally separated agar plates doubled lateral root length without having a differential effect on lateral root number. In the Fe uptake-defective mutant *iron-regulated transporter1 (irt1)*, lateral root development was severely repressed, but a requirement for IRT1 could be circumvented by Fe application to shoots, indicating that symplastic Fe triggered the local elongation of lateral roots. The Fe-stimulated emergence of lateral root primordia and root cell elongation depended on the rootward auxin stream and was accompanied by a higher activity of the auxin reporter *DR5-β-glucuronidase* in lateral root apices. A crucial role of the auxin transporter AUXIN RESISTANT1 (AUX1) in Fe-triggered lateral root elongation was indicated by Fe-responsive AUX1 promoter activities in lateral root apices and by the failure of the *aux1-T* mutant to elongate lateral roots into Fe-enriched agar patches. We conclude that a local symplastic Fe gradient in lateral roots upregulates AUX1 to accumulate auxin in lateral root apices as a prerequisite for lateral root elongation.

INTRODUCTION

Lateral root formation is a postembryonic process (Dubrovsky et al., 2001) that starts with the priming of pericycle cells in the basal meristem of the parental root (De Smet et al., 2007). Upon activation by auxin, pericycle founder cells undergo a precisely coordinated sequence of divisions that gives rise to the lateral root primordium (Dubrovsky et al., 2001). Once established, the primordium can further develop and a lateral root can eventually emerge from the parental root. The plant hormone auxin appears to be a central player in the regulation of many developmental steps required for lateral root formation (Casimiro et al., 2001; Fukaki et al., 2007; Péret et al., 2009). As a consequence of such a key role, many mutants defective in auxin transport and signaling show defects in lateral root development (Fukaki et al., 2002; Marchant et al., 2002; Geldner et al., 2004; Okushima et al., 2007; Wu et al., 2007). All developmental steps are genetically programmed and some are highly responsive to environmental cues.

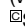
Among the most critical environmental factors, nutrient availability can profoundly shape root architecture (López-Bucio et al., 2003; Hodge, 2006). Mild nitrogen (N), sulfur (S), or phosphorus (P) deficiency usually extends the root system and increases the root-to-shoot ratios (Marschner, 1995; López-Bucio et al., 2003), whereas a local supply of nitrate or phosphate to otherwise N- or P-deficient plants stimulates lateral root development (Drew, 1975; Zhang et al., 1999; Linkohr et al., 2002). Furthermore, a localized supply of nitrate or phosphate promotes lateral root elongation in *Arabidopsis thaliana*, whereas only local nitrate supply additionally increases lateral root density (Zhang et al., 1999; Linkohr et al., 2002). Thus, lateral root formation is affected by nutrients at different developmental stages (e.g., initiation versus elongation) and in a nutrient-specific manner. In the case of N, it has been shown that ammonium and nitrate have complementary effects on lateral root architecture, with ammonium mainly enhancing initiation and nitrate the elongation of lateral roots. In particular for ammonium, experimental evidence has been provided that lateral root initiation was not caused by a nutritional but rather by a sensing event (Lima et al., 2010). This promotes the concept that adaptations of primary or lateral root development to nontoxic nutrient supplies can be seen as a morphological readout for nutrient sensing. However, apart from N and P responses, our understanding of nutrient-dependent modulations of lateral root development and their interaction with hormonal signals remains poor.

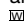
As lateral root growth shortens diffusion pathways of nutrients in the soil solution to the root surface, we hypothesized that profound changes in lateral root architecture should be expected for those nutrients that are sparingly soluble. In particular, the

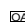
¹ These authors contributed equally to this work.

² Current address: Centro de Energia Nuclear na Agricultura, Universidade de São Paulo, Piracicaba, 13416-000 SP, Brazil.

³ Address correspondence to vonwiren@ipk-gatersleben.de. The author responsible for distribution of materials integral to the findings presented in this article in accordance with the policy described in the Instructions for Authors (www.plantcell.org) is: Nicolaus von Wirén (vonwiren@ipk-gatersleben.de).

 Some figures in this article are displayed in color online but in black and white in the print edition.

 Online version contains Web-only data.

 Open Access articles can be viewed online without a subscription. www.plantcell.org/cgi/doi/10.1105/tpc.111.092973

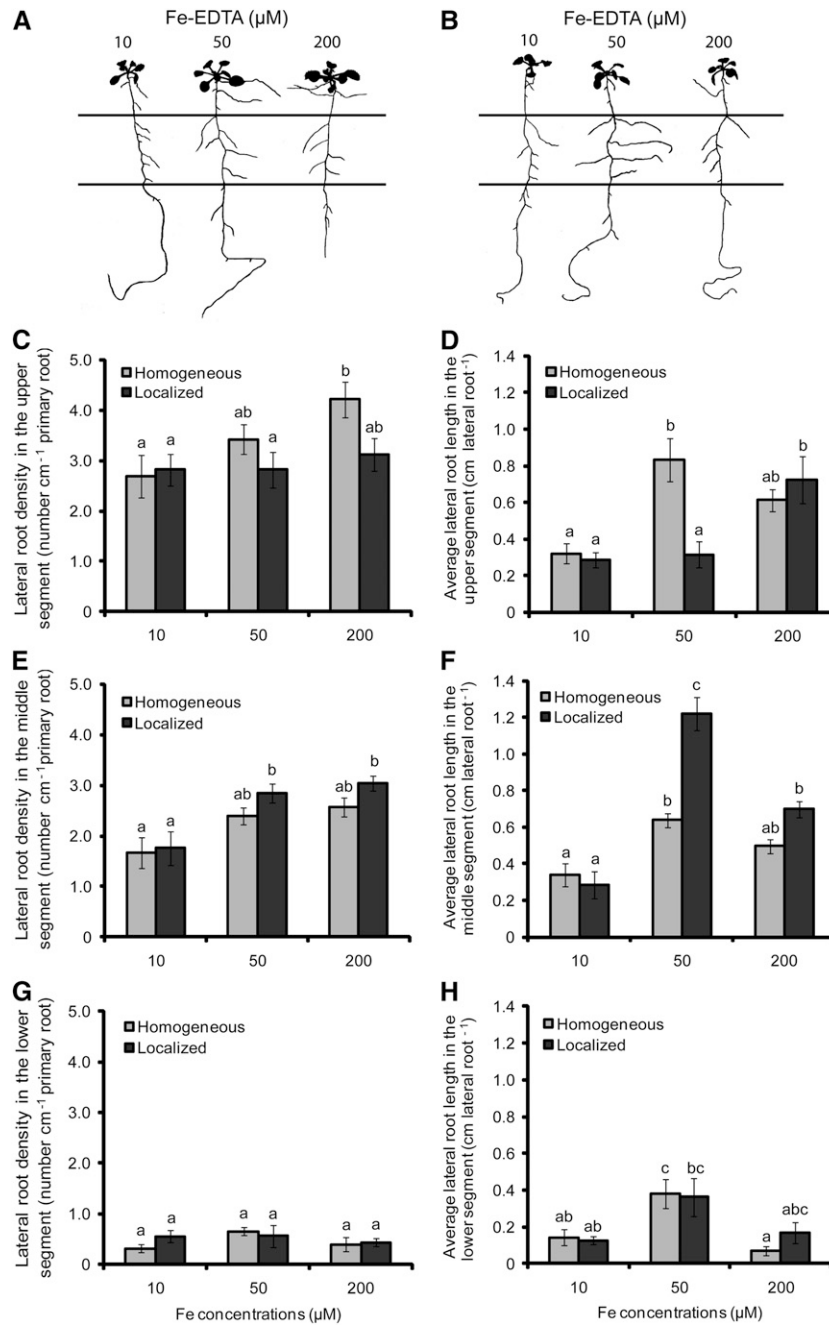


Figure 1. Effect of Homogeneous and Localized Fe Supplies on Lateral Root Development of *Arabidopsis* Plants.

(A) and (B) Root architecture of wild-type plants (accession Col-0) in response to Fe supply. Seedlings were grown on half-strength MS medium without Fe for 7 d before being transferred to SAPs containing half-strength MS and 75 μM ferrozine. Fe(III)-EDTA (μM) was added at the indicated concentrations to all three segments (A; homogeneous supply) or only to the middle segment (B; localized supply). Plants were scanned after 15 d of growth on Fe treatments, and representative plants are shown. Horizontal lines represent the borders between the three segments.

(C) to (H) Lateral root density (C, E, and G) and average lateral root length (D, F, and H) in the top (C and D), middle (E and F), and bottom (G and H) segment. Bars indicate means ± SE; n = 7 plates containing three plants. Different letters indicate significant differences among means (P < 0.05 by Tukey's test).

solubility of the micronutrient iron (Fe) is very low in well-aerated and alkaline soils but may locally increase (e.g., under reducing conditions in soil microsites) (Marschner, 1995). Since the distribution of organic matter and microbial activity and air- or water-conducting pores often occurs unevenly in soils, Fe availability varies locally and changes in a gradual or patchy pattern within the root zone (Hinsinger et al., 2005). Reports of morphological changes of the root system in response to varying Fe availabilities mostly refer back to earlier work and describe exclusively adaptations to Fe deficiency (Römheld and Marschner, 1981; Landsberg, 1986). Fe deficiency also induces the ectopic formation of root hairs (Schmidt et al., 2000) by modulating the length, position, and abundance of root hairs (Perry et al., 2007). Moreover, low Fe availability frequently leads to the formation of branched root hairs (Müller and Schmidt, 2004) through a signaling cascade that probably involves auxin and ethylene (Schmidt et al., 2000; Schmidt and Schikora, 2001). In contrast with morphological responses, physiological adaptations to low Fe availabilities have been extensively described, with a plasma membrane-localized H⁺-ATPase, the membrane-bound ferric Fe(III) reductase FRO2, and the divalent metal cation transporter IRON-REGULATED TRANSPORTER1 (IRT1) being major components of an Fe deficiency-inducible strategy for enhanced Fe acquisition in *Arabidopsis* (Giehl et al., 2009). Both *IRT1* and *FERRIC REDUCTION OXIDASE2 (FRO2)* are rapidly upregulated under Fe starvation via the basic helix-loop-helix transcription factor FER-LIKE IRON DEFICIENCY INDUCED TRANSCRIPTION FACTOR (FIT; Bauer et al., 2007). *FIT*, in turn, is also upregulated in response to Fe deficiency, suggesting that the Fe-sensing event acts upstream of this transcription factor (Colangelo and Guerinot, 2004; Jakoby et al., 2004). Resupply of Fe to Fe-starved plants induces *IRT1* and *FRO2* expression within 24 h, showing that Fe acts in the short term as an inducer of both genes (Vert et al., 2003). When plants were grown in a split-root setup, the expression of *IRT1* and *FRO2* was enhanced in the Fe-supplied but not in the Fe-deficient root parts, indicating that these components of Fe acquisition were subject to both a systemic and a local regulation (Vert et al., 2003). The relationship between these physiological and morphological adaptations of the root system to varying Fe availabilities is unclear.

To better understand the responses of the root system to varying Fe availabilities, we investigated changes in lateral root architecture in response to localized Fe supply in wild-type and mutant plants defective in Fe acquisition or translocation. Also considering Fe delivery from shoots, we identified that lateral root elongation is highly responsive to local Fe and that the symplastic Fe pool in lateral roots favors local auxin accumulation. We further identified the auxin transporter AUX1 as a major Fe-sensitive component in the auxin signaling pathway that mainly directs the rootward auxin stream into lateral roots that have access to Fe.

RESULTS

Localized Supply of Fe Stimulates Lateral Root Development in *Arabidopsis*

To investigate changes in root architecture of *Arabidopsis* in response to Fe deficiency, we first grew wild-type plants (Columbia-0 [Col-0]) on Fe-deficient half-strength Murashige and Skoog (MS) agar medium. Traces of Fe arising from inevitable Fe contamination by nutrient salts in the agar medium were inactivated by the addition of the Fe(II)-chelator ferrozine. When shoots of Fe-deficient plants turned chlorotic, primary root length was not affected (see Supplemental Figures 1A to 1C online), whereas lateral root density and average lateral root length strongly decreased (see Supplemental Figures 1D and 1E online). This observation showed that lateral root architecture in particular depends on the Fe nutritional status of the plant or on the external availability of Fe.

In an effort to monitor lateral root responses to local Fe availabilities, plants were grown on segmented agar plates (SAPs; Zhang and Forde, 1998), to which increasing concentrations of Fe(III)-EDTA were supplied either to all three segments (homogeneous supply) or only to the middle segment (localized supply). When plants were grown in a wide range of Fe concentrations, localized Fe supply significantly increased average lateral root length in the middle compartment in an optimum dose-response curve with a maximum at 50 μM Fe (see Supplemental Figure 2A online). By contrast, lateral root density did

Table 1. Concentration of Nutrients in Shoots of *Arabidopsis* (Accession Col-0) Plants Grown for 15 d under Different Concentrations of Fe, Supplied Either Homogeneously across All Three Segments (Homogeneous) or Only in the Middle Segment (Localized)

Fe Concentrations (μM)	Ca	K	Mg	P	S	Fe	Mn	Zn
Homogeneous supply								
10	5.64 \pm 0.7 ^{ab}	61.60 \pm 8.1 ^b	2.28 \pm 0.15 ^{ab}	13.30 \pm 0.7 ^a	17.35 \pm 0.9 ^b	66.8 \pm 0.4 ^a	272.0 \pm 57 ^b	669.5 \pm 30 ^{bc}
50	5.09 \pm 0.9 ^{ab}	55.80 \pm 1.1 ^{ab}	1.94 \pm 0.14 ^a	15.58 \pm 1.3 ^a	10.78 \pm 0.5 ^a	128.5 \pm 6.6 ^b	137.8 \pm 16 ^a	250.0 \pm 19 ^a
200	4.50 \pm 0.5 ^a	58.61 \pm 0.9 ^{ab}	1.81 \pm 0.08 ^b	16.07 \pm 2.0 ^a	9.77 \pm 0.7 ^a	154.8 \pm 24.8 ^b	127.7 \pm 11 ^a	173.0 \pm 27 ^a
Localized supply								
10	6.95 \pm 1.6 ^b	67.32 \pm 9.9 ^b	2.60 \pm 0.58 ^b	14.20 \pm 1.4 ^a	21.20 \pm 2.8 ^c	52.0 \pm 8.1 ^a	317.5 \pm 81 ^b	831.0 \pm 22 ^c
50	4.47 \pm 0.3 ^a	53.75 \pm 2.4 ^a	1.95 \pm 0.09 ^a	14.55 \pm 0.9 ^a	11.75 \pm 1.4 ^a	124.4 \pm 35.2 ^b	145.5 \pm 15 ^a	397.8 \pm 15 ^{ab}
200	4.67 \pm 1.0 ^{ab}	52.43 \pm 1.6 ^a	1.91 \pm 0.24 ^a	13.37 \pm 1.0 ^a	9.86 \pm 0.5 ^a	148.7 \pm 30.0 ^b	131.3 \pm 22 ^a	239.7 \pm 16 ^a

Shown are means and \pm SE ($n = 4$ replicates of 10 shoots). Different letters indicate significant differences among means ($P < 0.05$ by Tukey's test). Concentrations of Ca, K, Mg, P, and S are given in mg g^{-1} , while the concentrations of Fe, Mn, and Zn are in $\mu\text{g g}^{-1}$.

not differ significantly between the two modes of Fe supply (see Supplemental Figures 2B online). We then focused our analysis on three concentrations of localized Fe supply: 10, 50, and 200 μM Fe, which represented nonpromoting, inductive, and repressive effects on lateral root elongation, respectively. Improved plant development under increasing Fe supply was accompanied by a continuous increase in shoot chlorophyll levels and in lateral root density, irrespective of whether Fe was supplied homogeneously or locally (Figures 1A to 1C, 1E, and 1G; see Supplemental Figures 2B and 2C online). However, a differential response was observed for lateral root length. Relative to 10 μM Fe, 50 μM localized Fe enhanced average lateral root length by fourfold, resulting in a twofold higher value than under homogeneous supply (Figures 1B and 1F). With a further increase in the local Fe supply to 200 μM , lateral root length decreased to the level of plants grown under homogeneous Fe supply. Importantly, the enhanced lateral root elongation in response to localized supply of 50 μM Fe was restricted to the Fe-treated agar segment (Figures 1B and 1F), since no such response was observed in the upper or lower Fe-deficient segments (Figures 1D and 1H). Lateral root density in the middle segment was also stimulated by increasing localized Fe supply from 10 to 50 μM , but in contrast with lateral root length, it was not negatively affected in the presence of 200 μM Fe (Figure 1E). Lateral root length and density as well as chlorophyll concentrations showed no significant changes when Fe(III) was chelated by *N,N*-di-(2-hydroxybenzoyl)-ethylenediamine-*N,N*-diacetic acid instead of EDTA (data not shown), two chelating agents with distinct affinities for Fe and other metal micronutrients (Chaney, 1988). Therefore, the observed changes in root architecture were not due to an indirect effect of the Fe(III)-chelating agent and/or interactions of the chelator with other micronutrients. Taken together, these data indicated that the average lateral root length responded with more sensitivity to changes in localized Fe supply than did lateral root density or number.

Influence of the Mode of Fe Supply on the Nutritional Status of the Shoot

To address the question of whether enhanced lateral root elongation in the Fe-treated segment confers an advantage to plants growing under low Fe availabilities, we determined the chlorophyll concentration as a measure of the Fe nutritional status of the shoot (Morales et al., 1990). Chlorophyll levels reached maximum values at 50 μM Fe under either mode of Fe supply (see Supplemental Figure 2C online), indicating that an enhanced elongation of lateral roots into the Fe-containing patch enabled the plants to meet the Fe demand of their shoots even if Fe supply is spatially restricted. Moreover, the mode of Fe delivery did not significantly affect the shoot concentrations of Fe or other nutrients, since mineral element concentrations that were altered with increasing Fe supply showed similar changes under homogeneous and localized Fe treatment (Table 1). Thus, the shoot nutrient profile indicated that the morphological changes observed in the roots were not due to an undesirable effect of the mode of Fe supply on the accumulation of other essential macro- or microelements.

To verify the importance of lateral root development on Fe acquisition under local Fe supply, we employed the *arf7 arf19*

double mutant that is severely impaired in lateral development (Okushima et al., 2007). At 50 μM localized Fe supply, wild-type plants showed maximum lateral root elongation (see Supplemental Figure 2B online) and healthy growth with green leaves (Figures 2A and 2B). By contrast, young leaves of *arf7 arf19* plants turned chlorotic, indicative of an inadequate Fe nutritional status, and accumulated less chlorophyll (Figures 2A and 2B). Leaf chlorosis was not observed in *arf7 arf19* plants grown under a homogeneous supply of 50 μM Fe. This observation supported the view that the ability of roots to laterally explore Fe-enriched nutrient patches can be crucial for meeting the Fe demand of the shoot.

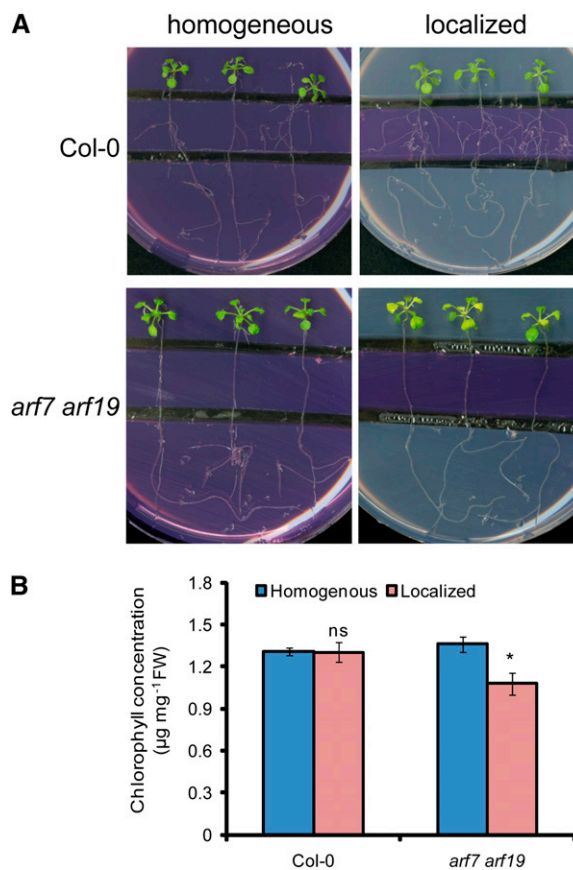


Figure 2. Defective Lateral Root Development in the *arf7 arf19* Double Mutant Causes Leaf Chlorosis under Localized Fe Supply.

(A) and (B) Wild-type (Col-0) and *arf7 arf19* seeds were germinated on Fe-free, half-strength MS medium for 7 d. Seedlings were then transferred to segmented agar plates supplied with 75 μM ferrozine and with 50 μM Fe-EDTA in all three segments (homogeneous) or only in the middle segment (localized).

(A) Photographs were taken after 15 d of treatments, and representative plants are shown.

(B) Chlorophyll concentrations of whole shoots of wild-type and *arf7 arf19* plants grown under homogeneous or localized supply of 50 μM Fe. Bars represent means \pm SE; $n = 6$ plates containing three plants. Asterisk denotes a significant difference according to Student's *t* test ($P < 0.05$). FW, fresh weight; ns, not significant.

Influence of FIT and IRT1 on Lateral Root Development under Localized Fe Supply

In *Arabidopsis*, many of the physiological Fe stress responses in roots are regulated by the transcription factor FIT (Colangelo and Guerinot, 2004; Jakoby et al., 2004). Interestingly, the tomato (*Solanum lycopersicum*) ortholog of FIT, Le FER, has been shown to additionally affect root hair formation (Ling et al., 2002). Thus, we assessed the involvement of this Fe-regulated transcription factor in root architectural changes in response to localized Fe supply. In *fit* mutant plants, the lateral root density was significantly lower than in wild-type plants at concentrations of up to 50 μM of localized Fe supply and achieved a similar number only at 200 μM Fe, while lateral root length in *fit* plants was significantly reduced over the whole range of locally supplied Fe concentrations (Figures 3A and 3B). To investigate whether FIT

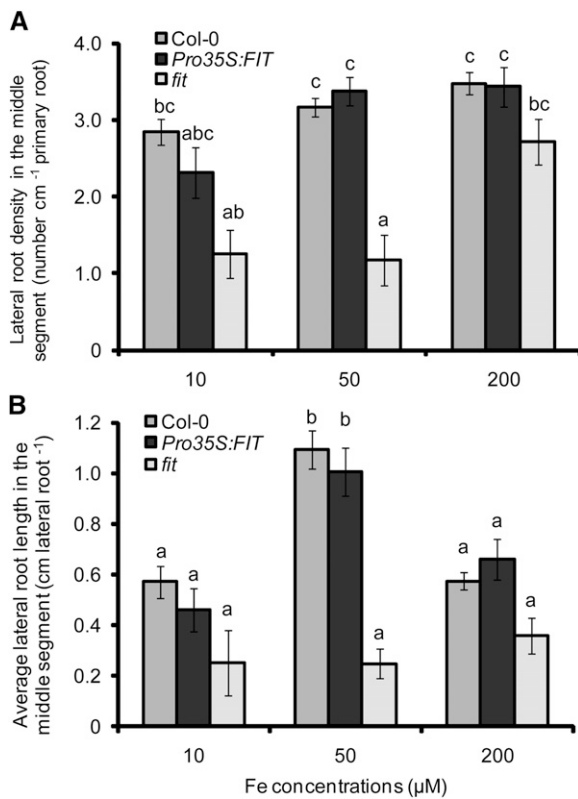


Figure 3. Lateral Root Development in Response to Localized Fe Supply in Transgenic Plants with Deregulated Expression of FIT.

Lateral root density (A) and average lateral root length (B) in wild-type (Col-0), *Pro35S:FIT*, and *fit* mutant plants as affected by the Fe concentration supplied to the middle segment. Seeds were germinated on Fe-free, half-strength MS medium for 7 d. Then, seedlings were transferred to segmented agar plates supplied with Fe in the middle segment at the indicated concentrations. After 15 d, the number of visible lateral roots (>0.5 mm) and mean lateral root length in the middle segment were determined by image analysis. Bars indicate means \pm SE, $n = 7$ to 12 plates with three plants per plate. Different letters indicate significant differences among means ($P < 0.05$ by Tukey's test).

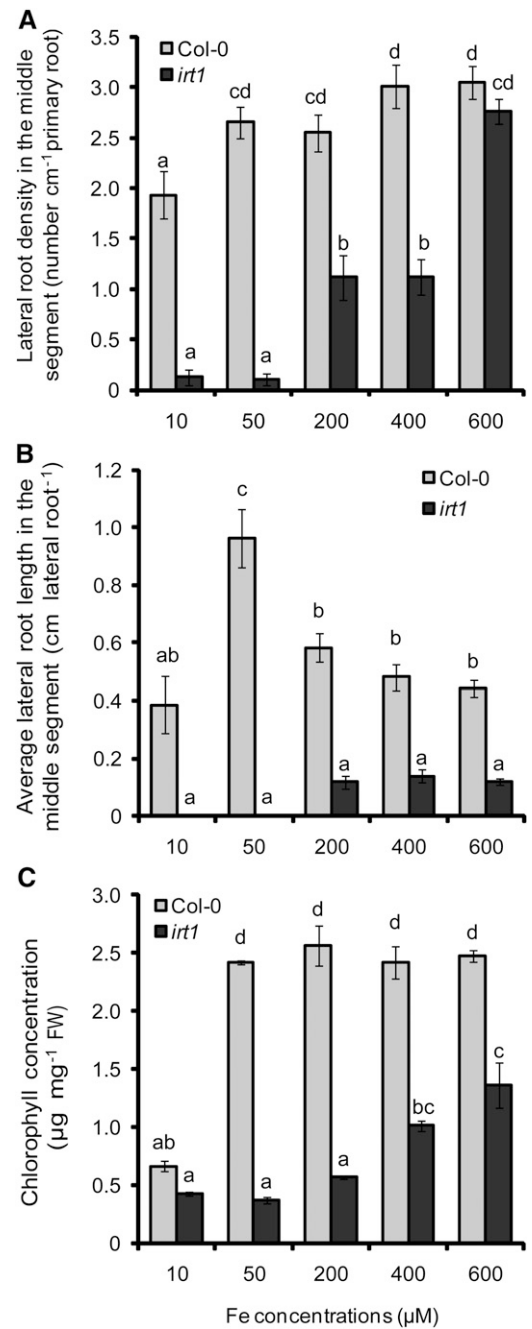


Figure 4. Lateral Root Development in Wild-Type and *irt1* Plants in Response to Localized Fe Supply.

Density (A) and average length (B) of lateral roots in wild-type (Col-0) and *irt1* mutant plants as affected by the Fe concentration supplied to the middle segment. Wild-type and *irt1* seeds were germinated on Fe-free, half-strength MS medium for 7 d. Seedlings were then transferred to segmented agar plates supplied with Fe in the middle segment at the indicated concentrations. After 15 d, the number and average length of visible lateral roots (>0.5 mm) in the middle segment were determined by image analysis. Shoot chlorophyll concentrations were determined after 15 d of growth (C). Bars represent means \pm SE; $n = 7$ replicates consisting of three plants. Different letters indicate significant differences among means ($P < 0.05$ by Tukey's test).

overexpression can provoke an altered morphological response, *Pro35S:FIT* plants were tested for lateral root formation under local Fe supply. However, the constitutive expression of *FIT* did not significantly affect root architecture, either with respect to the number or the length of lateral roots (Figures 3A and 3B).

As *fit* plants suffer from impaired Fe uptake due to lower *IRT1* and *FRO2* expression (Colangelo and Gueriot, 2004), the failure of *fit* plants to increase lateral root length may reflect a role for *IRT1/FRO2*-dependent Fe acquisition in increasing lateral root length under localized Fe supply. We therefore investigated whether the Fe transporter *IRT1* was involved in the differential

regulation of number and length of lateral roots under localized Fe supply. Whereas wild-type plants achieved their maximum number of lateral roots at 50 μM Fe, *irt1* plants developed few lateral roots below 200 μM Fe supply and achieved a similar number as wild-type plants only when 600 μM Fe was added to the middle segment (Figure 4A). By contrast, lateral root length in *irt1* mutant plants could not be restored to wild-type levels, even if Fe concentrations as high as 600 μM were supplied (Figure 4B). As a consequence, *irt1* shoots were chlorotic, with chlorophyll concentrations remaining below wild-type levels (Figure 4C), supporting the requirement for *IRT1* in the lateral root response to local Fe availabilities.

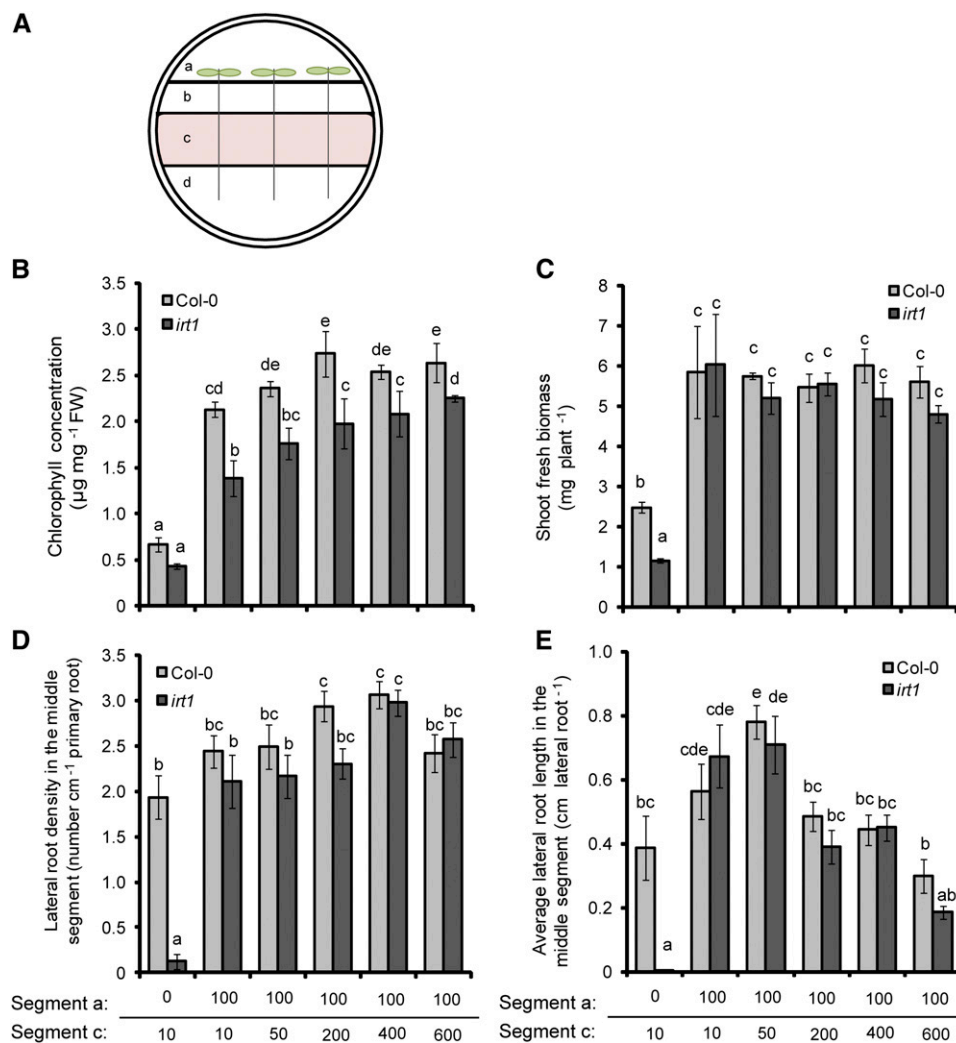


Figure 5. Effect of Shoot Fe Supply on the Development of Lateral Roots in Wild-Type (Col-0) and *irt1* on a Tetrapartite Agar Plate.

(A) Experimental setup for supplying Fe to shoots. Segment a was supplemented with 100 μM citrate or 100 μM Fe(III)-citrate, segment c was supplied with 10 to 600 μM Fe-EDTA, and segments b and d were Fe deficient.

(B) to (E) Chlorophyll concentrations (B), shoot biomass (C), density (D), and average length (E) of lateral roots of wild-type (Col-0) and *irt1* plants after growth for 14 d under increasing concentrations of Fe-EDTA in agar segment c. Bars indicate means \pm SE; $n = 6$ to 7 plates with three plants each. Different letters indicate significant differences among means ($P < 0.05$ by Tukey's test). FW, fresh weight.

[See online article for color version of this figure.]

Influence of Shoot-Derived Signals on Fe-Dependent Lateral Root Development

We then tested whether shoot Fe is able to influence lateral root development by growing *irt1* and wild-type plants under localized Fe supply with a fourth separated agar segment that harbored the shoot and was supplemented with 100 μM Fe(III)-citrate (Figure 5A). In fact, shoot application of Fe(III)-citrate efficiently alleviated chlorosis and improved growth in wild-type and *irt1* plants (Figures 5B and 5C). While shoot Fe supply slightly enhanced lateral root density and length in the wild type, it completely restored lateral root development to wild-type levels in *irt1* (Figures 5D and 5E). Shoot Fe supply now allowed *irt1* plants to respond to further increasing Fe concentrations to the middle root segment in the same manner as wild-type plants (Figure 5E). Hence, Fe supply to the shoots could compensate for IRT1-dependent Fe uptake by roots.

Lateral root elongation was then monitored in all three root compartments to further specify the influence of shoot-derived Fe. In fact, Fe supply to the shoots increased average lateral root length in the upper Fe-free segment to a greater extent than in the middle segment of plants supplied by 10 μM Fe (see Supplemental Figures 3A and 3B online). Moreover, when shoots obtained Fe-citrate, Perl's staining of root Fe(III) was stronger than in roots without shoot Fe supply, especially in the upper and middle root segments (see Supplemental Figure 3D online). These observations were indicative of Fe being translocated from the shoots and contributing to the locally absorbed Fe. We conclude that lateral root elongation is subject to local regulation by the Fe concentration of the root tissue rather than by the concentration of externally supplied Fe.

To address the involvement of a shoot-derived signal in lateral root development by an independent approach, we used the *ferric reductase defective3* (*frd3-1*) mutant and its allelic mutant *manganese accumulator1* (*man1-1*; also known as *frd3-3*). Both mutants show a constitutive upregulation of the Fe acquisition machinery in roots, despite accumulating more Fe in the root than wild-type plants, which also held true under our growth conditions (see Supplemental Figure 4 and Supplemental References 1 online; Delhaize, 1996; Rogers and Guerinot, 2002; Green and Rogers, 2004). Lateral root development in wild-type and *frd3-1* plants was similar at any tested concentration of localized Fe supply (Figures 6A and 6B). Only at 1 μM Fe supply did *frd3-1* mutant plants develop approximately two lateral roots more in their Fe-treated root segments than did the corresponding wild type (Figure 6A), while lateral root length followed the same concentration-dependent pattern in both lines (Figure 6B). Thus, the differential response between number and length of lateral roots, as was observed in wild-type plants, remained conserved despite the loss of FRD3. A similar growth response was observed in *man1-1* (*frd3-3*) mutant plants (see Supplemental Figure 5 online). These observations gained importance when taking into account the chlorophyll levels, which reflected a significantly lower Fe nutritional status in the *frd3-1* mutant than in wild-type plants at >10 μM Fe supply (Figure 6C). Considering that Fe-deficient plants have been proposed to release a shoot signal that upregulates Fe acquisition mechanisms in roots (Grusak and Pezeshgi, 1996; Vert et al., 2003) and that elevated

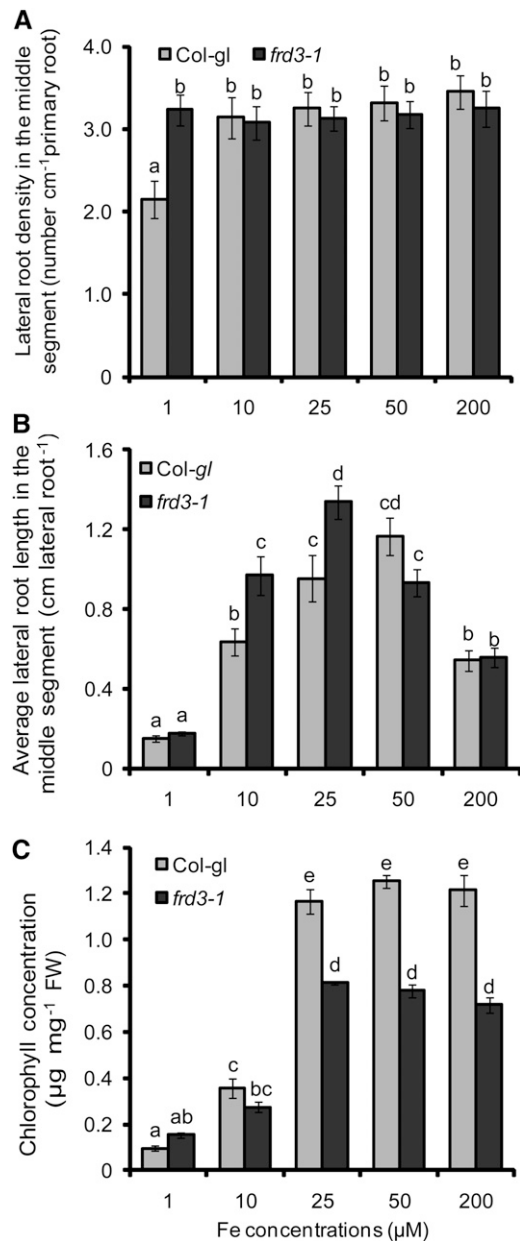


Figure 6. Lateral Root Development in Wild-Type and *frd3-1* Plants in Response to Localized Fe Supply.

Lateral root density (A), lateral root length (B), and chlorophyll concentration (C) in the shoots of wild-type (*Col-gl*) and *frd3-1* mutant plants. Seeds were germinated on Fe-deficient, half-strength MS medium for 7 d before transfer to segmented agar plates locally supplied with Fe(III)-EDTA only to the middle segment. Plant roots were scanned and the chlorophyll concentration determined after 15 d on Fe treatments. Bars represent means \pm SE; $n = 7$ to 12 plates with three seedlings per plate. Different letters indicate significant differences among means ($P < 0.05$ by Tukey's test). FW, fresh weight.

IRT1 mRNA levels in *frd3-1* roots confirmed a more severe Fe-deficient status (see Supplemental Figure 4A online), lateral root length at $\geq 25 \mu\text{M}$ Fe was expected to be derepressed in *frd3-1* mutants if this Fe deficiency signal from the shoot also regulates lateral root development. However, regarding the unaffected lateral root response in chlorotic *frd3-1* mutant plants (Figures 6A and 6B), evidence for the stimulation of Fe-triggered lateral root elongation by a shoot-borne Fe deficiency signal was not obtained.

We then addressed the question of whether the increased elongation of lateral roots exposed to Fe is subject to Fe-dependent regulation by other parts of the root system. Relative to localized Fe supply, expression levels of *IRT1* in homogeneously supplied roots from the middle segment remained lower (see Supplemental Figure 6 online), suggesting that a Fe satiety signal contributed to the downregulation of *IRT1*. In addition, the application of $50 \mu\text{M}$ Fe to root tips in the lower, Fe-free compartment was found to suppress lateral root elongation in the middle compartment (see Supplemental Figures 7A and 7B online). Taken together, these results indicate that Fe-stimulated lateral root elongation was independent of a *FRD3*-triggered Fe deficiency signal from the shoot but responded to Fe delivery from other parts of the root.

Effect of Localized Fe Supply on the Development of Lateral Roots

As localized Fe primarily affected the elongation of lateral roots (Figure 1), we assessed how lateral root primordia progressed during their development using transgenic *ProCYCB1;1:β-glucuronidase (GUS)* reporter lines (Ferreira et al., 1994), which allow the tracking of lateral root primordia before their emergence. We then exposed the primary root tip of Fe-deficient *ProCYCB1;1:GUS* seedlings to localized Fe supply and determined the developmental stages of preemerged lateral root initials after 3 and 6 d, according to the classification described by Malamy and Benfey (1997). At a homogeneous supply of $10 \mu\text{M}$ Fe (i.e., nonpromoting conditions for lateral root development), the number of emerged lateral roots started off at a rather high level (Table 2), probably due to higher tissue Fe concentrations relative to roots grown under a localized supply of $10 \mu\text{M}$ Fe. By contrast, at a 50 or $200 \mu\text{M}$ localized Fe supply, the

number of emerged lateral roots increased by more than three-fold compared with ~ 1.5 -fold under a homogeneous supply. From a developmental perspective, the rate of emergence of initiated lateral roots was increased by 56 or 40% under a localized supply compared with homogeneous Fe supply of 50 or $200 \mu\text{M}$, respectively (Table 2). These observations suggested that the local presence of Fe has a lower impact on the priming and initiation of lateral roots but stimulates the emergence and subsequent elongation of already initiated lateral root primordia.

The growth of primary and lateral roots is determined mainly by cell division in the mitotically active meristem and the differentiation and elongation of the cells that leave the meristem. To assess cell division activity within the meristems of lateral roots, we observed *ProCYCB1;1:GUS* expression and found that it was not considerably affected by the mode of Fe application when $50 \mu\text{M}$ Fe-EDTA was supplied (Figure 7A). However, under localized supply of 10 or $200 \mu\text{M}$ Fe, the activity of this cell cycle reporter was slightly reduced. To verify that Fe affects cell differentiation, meristem length was measured. Again, no marked difference was observed in the conditions tested, suggesting that neither the mode of Fe supply nor a difference in the Fe concentration affected cell differentiation (Figure 7B). However, the localized supply of $50 \mu\text{M}$ Fe significantly increased the length of individual rhizodermal cells (Figures 7A and 7C). No such effect was observed for the other two Fe concentrations tested or for $50 \mu\text{M}$ of a homogeneous Fe supply (Figure 7C). Thus, rather than affecting the meristem activity of lateral roots, localized Fe supply promotes the elongation of lateral root cells that leave the meristem.

Localized Fe Supply Alters Auxin Distribution in Lateral Roots

Lateral root growth is coordinately regulated by environmental and hormonal signals, among which auxin takes a central role in the regulation of all stages of lateral development (Casimiro et al., 2003; Fukaki and Tasaka, 2009; Péret et al., 2009). We therefore examined whether Fe availability affects auxin accumulation in lateral roots by analyzing the activity of the auxin-responsive synthetic promoter *DR5* (Ulmasov et al., 1997) under a homogeneous or localized supply of Fe. Whereas *DR5-GUS* signals were weak at 10 or $200 \mu\text{M}$ Fe irrespective of the mode of Fe supply, the supply of

Table 2. Number of Preemerged and Emerged Lateral Root Initials in Response to Homogeneous or Localized Fe Supply

Fe Concentrations (μM)	Preemerged	Emerged	Total	Rate of Emergence
Homogeneous supply				
10	1.0 ± 0.44	5.4 ± 0.81	6.4 ± 0.41	1.24
50	2.5 ± 0.42	3.6 ± 0.24	6.1 ± 0.38	1.03
200	2.8 ± 0.21	4.8 ± 0.20	7.6 ± 0.25	1.27
Localized supply				
10	3.0 ± 0.41	2.5 ± 0.87	5.5 ± 0.40	0.72
50	1.7 ± 0.33	5.5 ± 0.67	7.2 ± 0.48	1.61
200	1.8 ± 0.54	6.3 ± 0.42	8.1 ± 0.50	1.78

Lateral root initials of *ProCYCB1;1:GUS* plants were counted and classified according to Malamy and Benfey (1997) after 6 d of Fe treatments. Values represent means \pm SE; $n = 15$ to 20 seedlings. The rate of lateral root emergence (emerged lateral roots per day) was obtained by calculating the number of emerged lateral roots formed between 3 and 6 d after transfer to treatments.

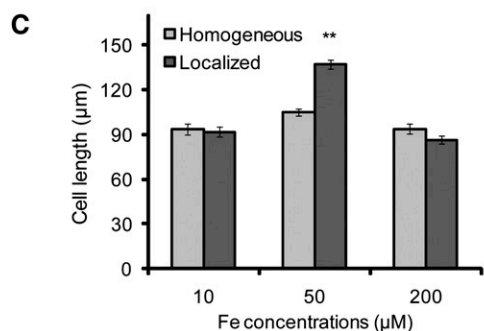
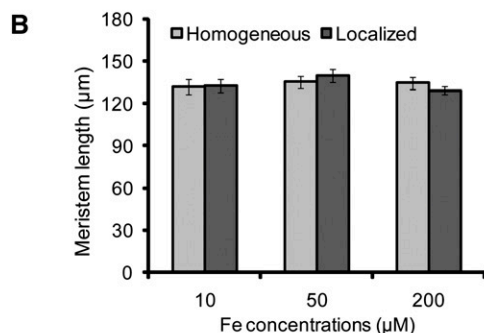
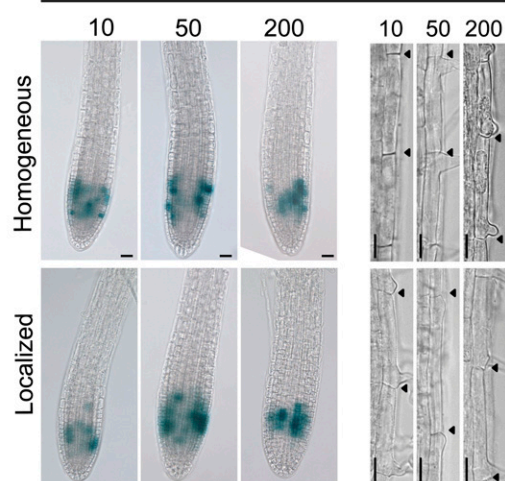
A Fe concentrations in the middle segment (μM)

Figure 7. Effect of Homogeneous or Localized Fe Supply on Cell Division, Differentiation, and Elongation.

(A) Seedlings of a *ProCYCB1;1:GUS* line were germinated on Fe-deficient medium and transferred to segmented agar plates supplemented with 75 μM ferrozine and with the indicated Fe(III)-EDTA concentrations only in the middle segment (localized supply) or in all three segments (homogeneous supply). After 7 d, lateral roots from the middle segment were assayed for GUS activity (**A**, left panel) and length of rhizodermal cells (**A**, right panel). Arrowheads indicate the boundaries of two consecutive epidermal cells. Bars = 25 μm .

(B) and **(C)** Length of lateral root meristems (**B**) and length of individual rhizodermal cells (**C**). Bars represent means \pm SE; $n = 3$ to 4 lateral roots from >14 seedlings. Asterisks denote a significant difference according to Student's *t* test ($P < 0.01$).

50 μM Fe only to the middle segment increased DR5-GUS activity in emerged and in elongated lateral root tips (Figures 8A and 8B). To identify the origin of the auxin, either leaves or primary root tips were treated with naphthylphthalamic acid (NPA), an inhibitor of polar auxin transport (Figure 8C). The application of NPA to leaves but not to the primary root tip reduced lateral root elongation of Fe-exposed lateral roots (Figure 8D). This indicated that the elevated auxin accumulation observed in Fe-treated lateral roots (Figures 8A and 8B) was mainly due to an enhanced rootward auxin transport rather than to an elevated shootward auxin transport or auxin biosynthesis in lateral root apices. Thus, locally supplied Fe favored the accumulation of auxin in lateral root tips. To determine whether this response indicated the existence of a signaling mechanism responsive to external or internal Fe concentrations, we compared *DR5-green fluorescent protein (GFP)* expression in wild-type (Col-0) and *irt1* plants grown under a localized supply of 50 μM Fe. Relative to the wild type, *DR5-GFP* expression in lateral root apices of the *irt1* mutant was markedly weaker in elongated lateral root tips (Figure 9). Similar patterns were also observed when 200 and 600 μM Fe were locally supplied to the roots (see Supplemental Figure 8 online). Importantly, Fe application to leaves not only restored lateral root elongation in *irt1* mutants (Figure 5E) but also restored auxin accumulation in lateral root apices to a large extent, as shown by the elevated *DR5-GFP*-dependent fluorescence (Figure 9). Altogether, these results indicated that, rather than external Fe, internal root Fe triggers the import and accumulation of shoot-derived auxin in lateral root apices.

Enhanced Elongation of Lateral Roots in Response to Local Fe Depends on AUX1

Since auxin distribution to lateral root tips depended on the mode of Fe supply (Figure 8), we examined the response of mutants defective in auxin biosynthesis (*nit1-3*), transport (*pin2-T*; *aux1-T*) or sensitivity (*tir1-T* and *axr1-3*) to local Fe supply. While lateral root length was increased in *pin2-T*, *nit1-3*, and *tir1-T* mutants to a similar extent as in wild-type (Col-0) plants, *axr1-3* and in particular *aux1-T* plants failed to show a significant stimulation of lateral root length under a local availability of 50 μM Fe (see Supplemental Figure 9 online).

Further considering the reported involvement of the auxin influx carrier AUX1 in lateral root development (Marchant et al., 2002; De Smet et al., 2007; Laskowski et al., 2008), we assessed its role in Fe-dependent changes in root architecture. As expected, *aux1-T* plants showed a reduced number of lateral roots (Figure 10A; Marchant et al., 2002), irrespective of the Fe treatments imposed. In contrast with wild-type plants that underwent an 80% increase in mean lateral root length when grown under localized supply of 50 μM Fe, *aux1-T* plants were not able to significantly increase lateral elongation (Figure 10B; see Supplemental Figure 9 online). On the other hand, 200 μM Fe suppressed lateral root elongation to a similar extent in both genotypes (Figure 10B), indicating that the loss of *AUX1* expression prevented an Fe-dependent increase in lateral root elongation in response to localized Fe. Recently, it has been shown that Fe deficiency triggers an overaccumulation of indole-3-acetic acid (IAA) and that *aux1-7* mutant plants exhibit reduced ferric chelate reductase activity under low Fe (Chen et al., 2010). When

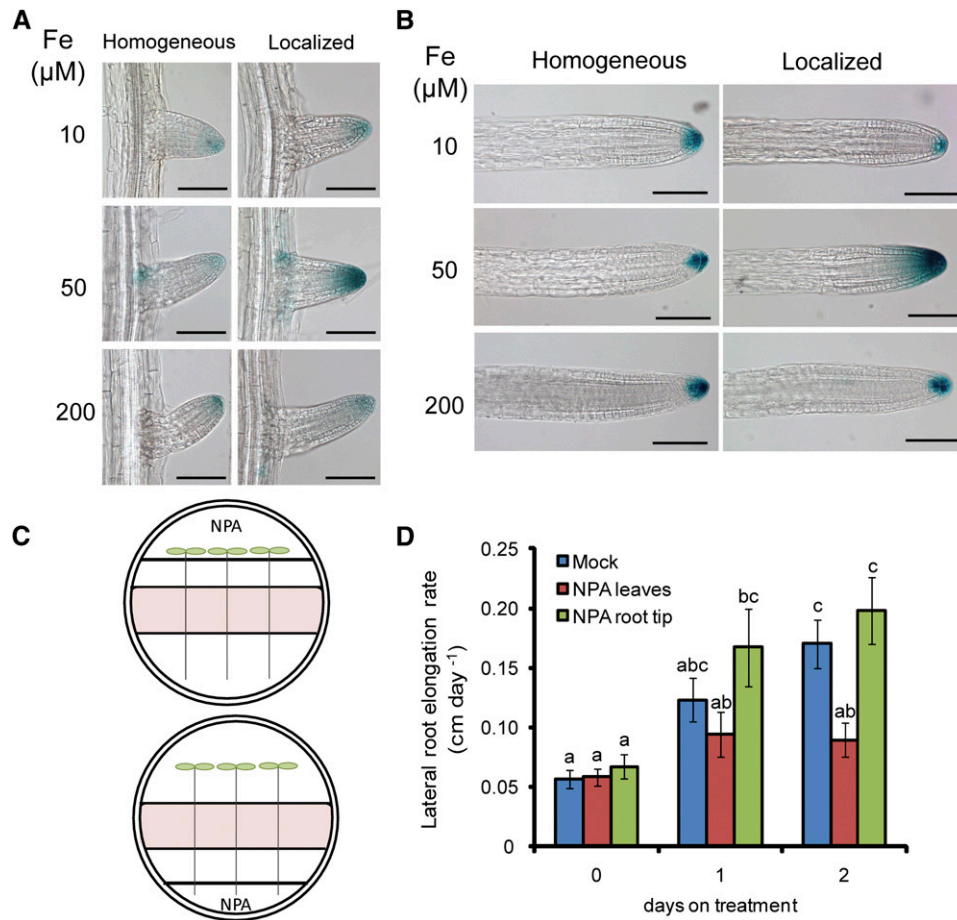


Figure 8. Role of Auxin in Fe-Dependent Lateral Root Elongation.

(A) and **(B)** Expression of the auxin-responsive reporter *DR5-GUS* in emerged **(A)** and elongating **(B)** lateral roots. Fe-EDTA (10, 50, or 200 μM) was supplied either homogeneously to all three agar segments or locally to the middle agar segment. Lateral roots were analyzed by light microscopy after 7 d of treatments ($n > 10$ seedlings). The experiments were repeated twice and representative lateral roots are shown. Bars = 100 μm .

(C) Experimental setup for supplying NPA either to leaves or to the primary root tip.

(D) Elongation rate of lateral roots of wild-type (Col-0) plants supplied locally with 50 μM Fe and treated with the auxin transport inhibitor NPA on leaves or on the primary root tip. Seeds were germinated on Fe-free, half-strength MS medium for 7 d. Seedlings were then transferred to segmented agar plates supplied with 50 μM Fe in the middle segment and on which the shoot or the primary root tip was placed over a fourth segment. After 7 d, 5 μM NPA was supplied either to the leaves or to the primary root tip. Lateral root length was measured every day from days 6 to 9 to determine lateral root growth rate before and after NPA treatments. Bars indicate means \pm SE; $n = 6$ plates with three plants each. Different letters indicate significant differences among means ($P < 0.05$ by Tukey's test).

we measured ferric chelate reductase activity in *aux1-T* roots with a homogeneous or localized supply of 50 μM Fe, no significant difference was observed, indicating that the missing stimulation of lateral root elongation in response to local Fe in *aux1-T* plants was not related to a compromised Fe(III) reduction at the root surface (see Supplemental Figure 10 and Supplemental References 1 online).

To establish whether *AUX1* expression is regulated by local Fe, we first measured its expression levels by means of quantitative RT-PCR. However, no significant difference in *AUX1* expression levels could be detected in roots sampled from the middle agar segment of plants grown under homogeneous or localized Fe supply (data not shown). We thus monitored *AUX1* expression in

lateral roots by employing *ProAUX1:AUX1:yellow fluorescent protein (YFP)* lines. The localized supply of 50 μM Fe markedly increased *AUX1*-dependent fluorescence in the apex of emerged lateral roots (Figure 10C). In fact, quantification of *AUX1*-derived fluorescence confined to the lateral root apex revealed that the localized supply of 50 μM Fe to the middle segment increased the *AUX1* signal intensity by $>30\%$ relative to a homogeneous supply (Figure 10D). In these lateral roots, *AUX1*-dependent fluorescence expanded basally. A localized supply of 10 or 200 μM Fe had no impact on the relative intensities of *ProAUX1:AUX1:YFP*-derived fluorescence compared with a homogeneous supply of the same Fe concentrations (Figure 10D). Remarkably, the *AUX1* reporter was highly responsive to a local supply of Fe, since its increase

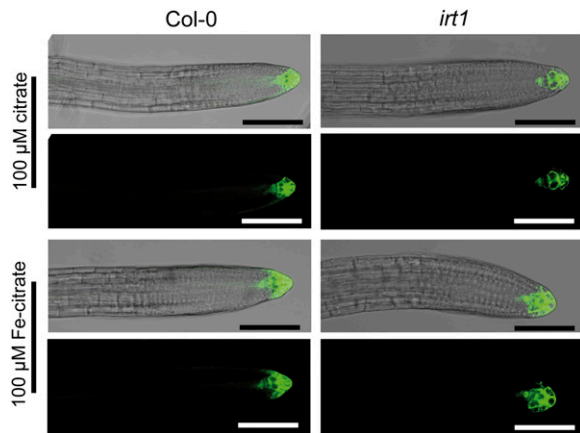


Figure 9. Auxin Accumulation Responds to Internal Fe Levels of the Root.

Expression of the auxin-sensitive reporter *DR5-GFP* in lateral roots of wild-type (Col-0) and *irt1* plants in response to localized supply of 50 μM Fe and the concomitant shoot supplementation of 100 μM citrate or Fe-citrate. Seven-day-old seedlings germinated on Fe-deficient medium were transferred to segmented agar plates containing 50 μM Fe-EDTA in the middle segment. Lateral roots were analyzed by confocal laser scanning microscopy after 7 d of treatments ($n > 10$ seedlings). The experiments were repeated twice, and representative lateral roots are shown. Bars = 100 μm .

[See online article for color version of this figure.]

was restricted to the middle, Fe-containing compartment (Figure 10E). Taken together, these results indicated that a localized availability of Fe stimulates lateral root elongation by increasing AUX1 expression and subsequent auxin accumulation in the lateral root apex.

DISCUSSION

Plant root development strongly depends on nutrient availability, and changes in the root system architecture are mostly characterized by a differential growth response of root organs in a nutrient-specific or even nutrient form-specific manner. The observation that localized nitrate supply mainly stimulated lateral root elongation while ammonium stimulated lateral root initiation (Remans et al., 2006; Lima et al., 2010) indicated that individual steps in root development respond to nutrients with a differential sensitivity. In the search for further nutrients that trigger lateral root responses, we observed a particular strong impact of a spatially restricted Fe availability in the root tissue on the elongation of lateral root cells. With the Fe-dependent regulation of AUX1, this study identified another link between the integration of nutrient signals and the developmental programs of root formation.

Localized Fe Supply Differentially Regulates Lateral Root Density and Lateral Root Length

The localized availability of Fe exerted a dual effect on lateral root development in *Arabidopsis*. First, a direct comparison of lateral root growth responses to homogeneous or localized supply of Fe

in the middle segment revealed a twofold increase in average lateral root length of wild-type plants grown on a 50 μM localized Fe supply relative to plants grown on a homogeneous Fe supply, while lateral root density was much less affected (Figures 1E and 1F). This increase in lateral root length was caused by enhanced cell elongation rather than by stimulated cell division or differentiation (Figure 7). However, during the early stages of development, lateral root primordia of plants exposed to 50 or 200 μM localized Fe emerged more quickly (Table 2). This suggests that, at this developmental stage, Fe may additionally stimulate cell division and/or differentiation. In the case of localized nitrate supply, stimulated lateral root elongation was indirectly assigned to increased cell production rates in the lateral root tip, since cell length was not affected (Zhang et al., 1999). This indicates that nitrate and Fe ultimately affect lateral root formation at different developmental stages. Secondly, high local Fe supplies evoked an inhibition of lateral root length (Figures 1F and 4B) but not of lateral root density (Figures 1E and 4A). Irrespective of the mode of Fe supply, lateral root density was maximally stimulated at ≥ 25 μM Fe and did not decrease even at excessive Fe supplies (see Supplemental Figure 2 online), suggesting that Fe triggered lateral root initiation whenever a certain threshold level was reached. Such a response would be expected if Fe just fulfilled a nutritional role. By contrast, the sharply defined optimum dose-response curve observed for lateral root length pointed to a Fe-sensitive regulatory component acting within a permissive concentration range, far below those Fe supplies that repress growth (Figure 4B; see Supplemental Figure 2A online). As lateral root length was also repressed by Fe supply to the root tip (see Supplemental Figure 7 online), we conclude that locally accumulated Fe in the root tissue is integrated with a Fe satiety or deficiency signal from other root parts to adjust lateral root elongation. This behavior is more indicative of a sensing response (i.e., a signaling event triggered by the nutrient apart from its metabolic function).

The Local Regulation of Lateral Root Development by Fe

To improve Fe acquisition from the rhizosphere, *Arabidopsis* plants induce strategy I responses consisting of enhanced proton extrusion, Fe^{3+} reduction, and Fe^{2+} uptake (Kim and Gueriot, 2007). The expression of the corresponding genes, in particular *IRT1* and *FRO2*, is subject to a local regulation, in which Fe acts as a local inducer, and a systemic control, in which a shoot-derived Fe satiety signal represses gene expression (Vert et al., 2003; Giehl et al., 2009). Several lines of evidence from this study indicated that the impact of Fe on lateral root development is different and primarily subject to a root-endogenous rather than a shoot-dependent systemic regulation: (1) Lateral root elongation decreased at external Fe supplies of > 50 μM (Figure 1F; see Supplemental Figure 2A online), even though the Fe nutritional status of the shoots did not change (Table 1; see Supplemental Figure 2C online). This observation emphasizes that the Fe-dependent regulation of this morphological trait differs from that of physiological root traits, which are regulated by a long-distance Fe signal from the shoot (Vert et al., 2003; Lucena et al., 2006; Enomoto et al., 2007). (2) Under localized Fe supply, lateral root elongation in *frd3-1* mutants did not differ significantly

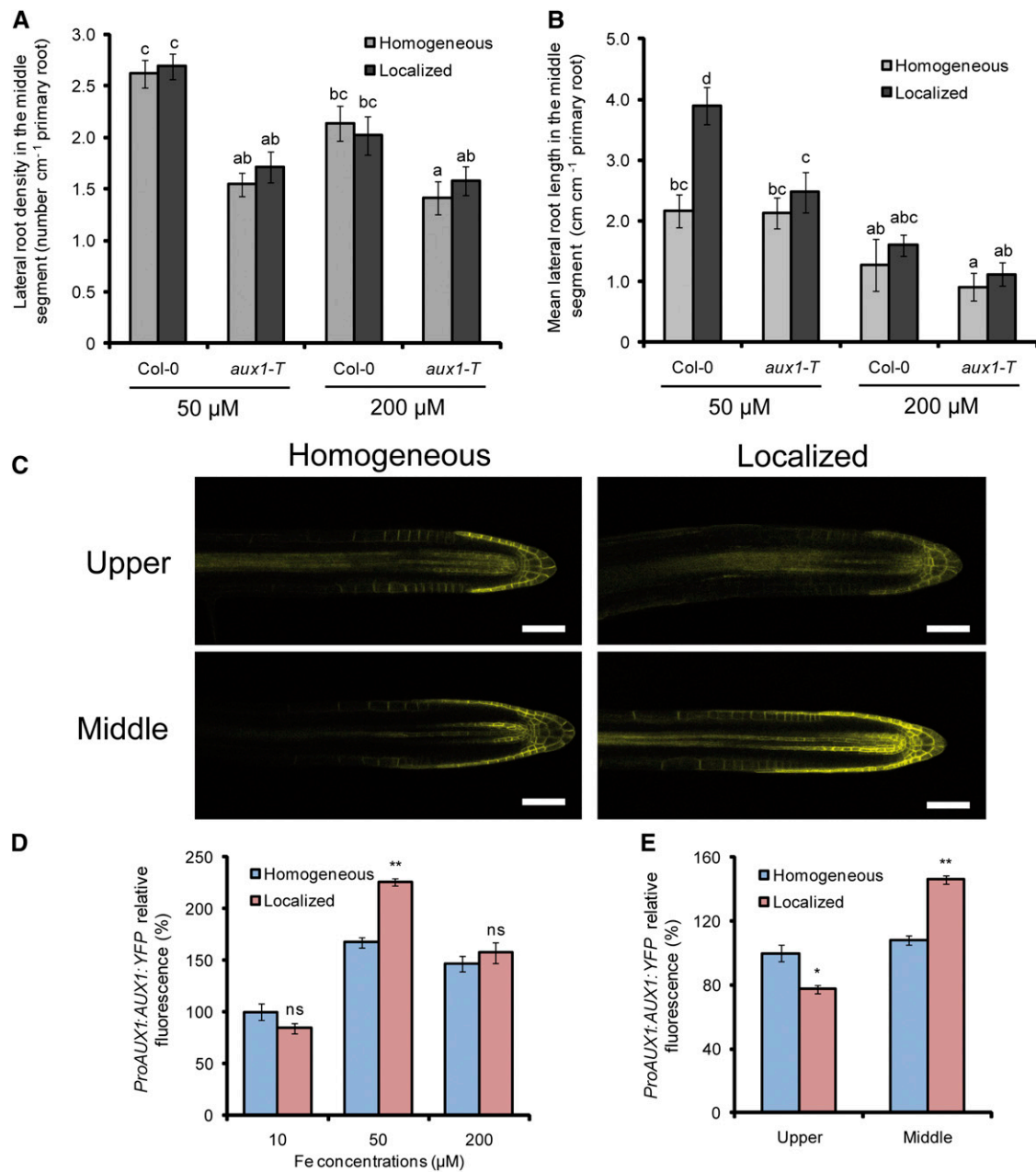


Figure 10. The Effect of Localized Fe on Lateral Root Elongation Is Dependent on AUX1.

(A) and **(B)** Density **(A)** and length **(B)** of lateral roots in wild-type (Col-0) and *aux1-T* plants after 15 d on treatments. Bars represent means \pm SE; $n = 7$ plates with three seedlings per plate. Different letters indicate significant differences among means ($P < 0.05$ by Tukey's test).

(C) *ProAUX1:AUX1:YFP* expression in lateral roots from the upper and middle segments in wild-type plants grown on a homogeneous or localized supply of 50 μ M Fe. Bars = 50 μ m.

(D) Relative YFP fluorescence in lateral root tips of plants grown under homogeneous or localized supply of 10, 50, or 200 μ M Fe.

(E) Relative YFP fluorescence in lateral root apices from the upper and middle segment of plants grown under homogeneous or localized supply of 50 μ M Fe. Bars represent means \pm SE; $n > 10$ seedlings. One asterisk and two asterisks denote a significant difference according to Student's *t* test at $P < 0.05$ or $P < 0.01$, respectively.

from that of wild-type plants, although *frd3-1* shoots suffered from Fe deficiency (Figures 6B and 6C). Since FRD3 acts as a citrate loader into the xylem required for root-to-shoot translocation of Fe, *frd3-1* plants accumulate Fe in roots while the shoot remains chlorotic (Durrett et al., 2007), thereby causing a weaker repression of strategy I responses in roots upon Fe resupply (Rogers and Guerinot, 2002). This was also the case in our split-root assay (Figure 6C; see Supplemental Figure 4 online), corroborating that lateral root elongation was independent of a Fe deficiency signal derived from chlorotic shoots. (3) Although the application of Fe to leaves stimulated lateral root elongation, this response was mainly restricted to the upper Fe-free segments which showed increased Fe levels (see Supplemental Figure 3 online), suggesting that Fe itself was translocated downwards to the root. In addition, Fe-citrate supply to leaves did not repress the stimulation of lateral root elongation under localized supply of 50 μ M Fe (Figure 5E). Collectively, these observations reinforce the view of a local regulation of lateral root elongation by Fe, although shoot-derived Fe can add up with externally available Fe to stimulate lateral root growth. (4) Elevated Fe supplies to *irt1* plants did not restore lateral root elongation to wild-type levels (Figure 4B), indicating that IRT1, which is preferentially expressed in the rhizodermis of Fe-deficient plants (Vert et al., 2002), functions as the major Fe transporter upstream of the Fe sensing event that triggers lateral root elongation. However, since the application of Fe-citrate to *irt1* shoots restored chlorophyll levels and lateral root elongation to wild-type levels (Figure 5), IRT1 is only an essential upstream component in eliciting this morphological response whenever the Fe demand of the root tissue is met by the uptake of external Fe.

AUX1-Mediated Auxin Accumulation Is Required for Fe-Dependent Lateral Root Elongation

Auxin is the central player in lateral root initiation and elongation (reviewed in Fukaki et al., 2007; Péret et al., 2009), and the following findings show how auxin signaling might be affected by nutrient supply at different developmental stages. Lateral root proliferation under P deficiency increases auxin sensitivity in pericycle cells by enhancing the expression of the auxin receptor TIR1 and degrading IAA/AUX repressors to trigger auxin signaling (Pérez-Torres et al., 2008). In the case of lateral root elongation under localized nitrate supply, a nitrate-dependent repression of the nitrate transporter NRT1.1 proceeds apical auxin accumulation in the lateral root apex and is a prerequisite for lateral root elongation (Krouk et al., 2010). Since *DR5* promoter activity was elevated under localized Fe supply (Figures 8A and 8B) but not at nonpermissive external Fe concentrations or in the *irt1* mutant defective in Fe uptake and Fe-mediated lateral root elongation (Figures 8B and 9), Fe-mediated lateral root elongation also appears to rely on auxin accumulation or sensitivity in the lateral root apex. Considering that the shoot supply of Fe-citrate can restore *DR5-GFP* expression in lateral roots of *irt1* (Figure 9) and circumvent the requirement for IRT1 in lateral root elongation (Figure 5), it is likely that symplastic Fe accounts for the auxin accumulation in lateral root tips.

Screening of auxin-related mutants for Fe-responsive lateral root elongation pointed to the auxin importer AUX1 as a candi-

date for integrating the local Fe nutritional status in auxin signaling (see Supplemental Figure 9 online). AUX1 has been implicated in both the shootward and rootward routes of auxin transport (Swarup et al., 2005; De Smet et al., 2007; Laskowski et al., 2008). Together with PIN2, AUX1 forms the basic machinery for shootward auxin transport (Swarup et al., 2001). Since *aux1-T* but not *pin2-T* mutants failed to elongate lateral roots in response to localized Fe (see Supplemental Figure 9 online), it is likely that rootward rather than shootward auxin transport into lateral roots represents the sensitive checkpoint for this Fe-dependent morphological response. In support of this hypothesis, the *aux1-T* mutant failed to increase lateral root length at a permissive concentration of local Fe supply (Figures 10A and 10B). Furthermore, only localized but not homogeneous Fe supply increased *ProAUX1:AUX1:YFP* expression levels in the lateral root meristems (Figures 10C and 10D). The increased AUX1 accumulation is likely to divert more auxin originating from the rootward auxin stream into Fe-exposed lateral roots (Figure 8D), which is supported by previous observations of low auxin reporter activities in lateral roots of *aux1* mutants (Sabatini et al., 1999; Bao et al., 2007; De Smet et al., 2007). Importantly, under localized Fe supply, the increased *ProAUX1:AUX1:YFP* expression was restricted to lateral roots exposed to Fe but low in lateral root apices grown on Fe-free medium (Figure 10E). Presuming an elevated proton-ATPase activity in the Fe-containing patch along

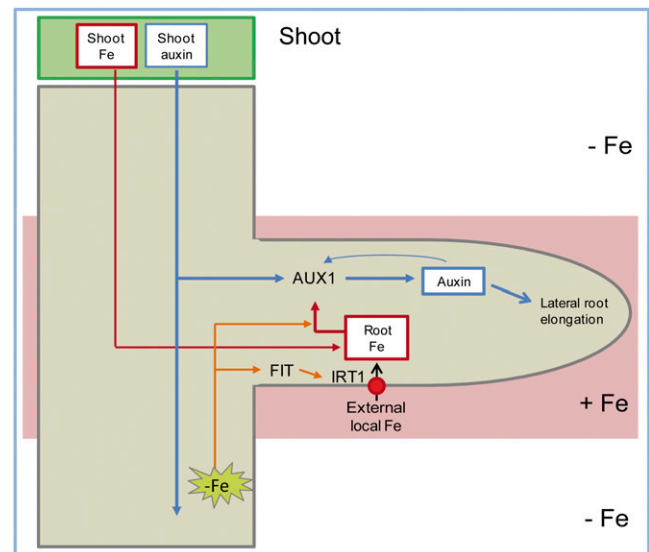


Figure 11. Model for the Regulation of Lateral Root Development under Localized Availability of Fe.

Uptake of Fe via the high-affinity Fe²⁺ transporter IRT1 increases the symplastic root Fe pool, which can be replenished by Fe derived from the shoot or other parts of the root. The local enrichment in symplastic root Fe leads to an upregulation of the auxin importer AUX1, which channels auxin from the rootward auxin stream toward the lateral root tip. This response is reinforced by the integration of systemic Fe deficiency signals from other parts of the root. Increased rootward auxin movement in lateral roots triggers the longitudinal elongation of mature cells, subsequently resulting in enhanced lateral root elongation.

[See online article for color version of this figure.]

with the induction of IRT1 (see Supplemental Figure 6 online), a lower apoplastic pH may additionally stimulate H⁺/IAA transport by AUX1. Since *AUX1* expression itself is induced by auxin (Laskowski et al., 2006, 2008; Lewis et al., 2011), it is likely that by facilitating auxin influx into Fe-treated lateral roots, AUX1 starts a positive feedback loop, in which increased auxin accumulation further induces additional AUX1 accumulation. Auxin regulates both lateral root initiation and elongation, but evidence is increasing that lateral root initiation primarily depends on the shootward auxin flow (Casimiro et al., 2001; De Smet et al., 2007), whereas lateral root emergence and elongation are regulated by the rootward auxin stream (Casimiro et al., 2001; Swarup et al., 2008). It is unclear at which level auxin affects cell elongation. One possibility is that shootward auxin transport ends up in the elongation zone, where it contributes to the auxin-dependent inhibition of cell elongation (Swarup et al., 2005). Interestingly, the loss of MDR1/PGP19/ABCB19, a multidrug resistance-like ABC transporter, leads to a significant reduction of rootward auxin transport within lateral roots and to decreased DR5-GUS activity, specifically in the apices of lateral roots (Lewis et al., 2007; Wu et al., 2007). As a consequence, *mdr1* mutants show impaired emergence and slower elongation of lateral roots. By contrast, the loss of MDR4/PGP4/ABCD4, which participates in the shootward transport of auxin (Lewis et al., 2007), had no effect on lateral root development (Wu et al., 2007), further emphasizing the importance of rootward auxin transport for lateral root elongation and development. Irrespective of whether shootward or rootward auxin streams have caused the observed Fe-triggered lateral root responses (Figure 1E), the induction of AUX1 under local Fe (Figures 10C and 10D) highlights the importance of AUX1 in lateral root elongation in response to environmental cues.

Based on our results, we propose a model for the Fe-dependent regulation of lateral root elongation under heterogeneous Fe availability (Figure 11). Root uptake of localized Fe is mainly mediated by the Fe²⁺ transporter IRT1 and builds up a symplastic Fe pool. This symplastic Fe pool can be replenished by Fe derived from the shoot or from the uptake by other root parts and establishes a local gradient in tissue Fe concentrations toward Fe-deficient root tissues. AUX1 expression increases in response to the local symplastic Fe pool, and this response probably integrates a Fe deficiency signal from other root parts. AUX1 facilitates auxin transport and accumulation, which further stimulates AUX1 expression and the emergence of initiated lateral root primordia as well as the elongation of emerged lateral roots, the latter being mainly the result of enhanced elongation of differentiated cells. Taken together, our findings provide an example of how the patchy availability of an essential microelement interferes with hormonal signaling to reprogram lateral root development for a more efficient acquisition of this microelement from the growth substrate.

METHODS

Plant Material and Growth Conditions

The wild-type (*Arabidopsis thaliana*) ecotypes used in this study were Col-0 and Col-*glabrous1* (Col-*gl*). The following and previously described

mutants and transgenic lines (in Col-0 background) were used: *aux1-1* (SALK_020355C; Fischer et al., 2006), *tir1-1* (SALK_151603C; Men et al., 2008), *pin2-1* (SALK_122916C), *irt1-1* (Col-0 background; Varotto et al., 2002), *fit-3* (Jakoby et al., 2004), *35S-FIT* (Jakoby et al., 2004), *Pro-CYCB1;1:GUS* (Ferreira et al., 1994), *DR5-GUS* (Ulmasov et al., 1997), *DR5-GFP* (Friml et al., 2003), *ProAUX1:AUX1:YFP* (Swarup et al., 2004), *axr1-3* (Lincoln et al., 1990), and *nit1-3* (Normanly et al., 1997). The *frd3-1* mutant was in the Col-*gl* background (Rogers and Guerinot, 2002). Seeds were surface sterilized in 70% (v/v) ethanol and 0.05% (v/v) Triton X-100. The seeds were planted on sterile plates containing half-strength MS medium (Murashige and Skoog, 1962) without Fe, supplemented with 0.5% Suc, 2.5 mM MES, pH 5.6, and 1% (w/v) Difco agar (Becton Dickinson). The 7-d-old seedlings were transferred to SAPs containing agar medium as described above and Fe(III)-EDTA at the indicated concentrations. Before agar segments were separated, the medium was supplemented with 75 μ M ferrozine [3-(2-pyridyl)-5,6-diphenyl-1,2,4-triazine sulfonate] (Serva) to render traces of Fe contaminants in the agar unavailable (Jain et al., 2009), ensuring a high reproducibility in consecutive experiments. Thus, all root responses recorded here were in fact initiated by lower Fe concentrations than those supplied to the medium. Three seedlings per plate were transferred to segmented plates with 3 mm of the primary root apex touching the top of the middle segment, oriented in a vertical position and cultured under a 22°C/19°C and 10/14-h light/dark regime at a light intensity of 120 μ mol photons m⁻² s⁻¹. To inhibit polar auxin transport, NPA was dissolved in DMSO and supplied to the fourth agar segment, where either the leaves or the primary root tip was placed (Figure 8C). The final concentration of NPA was 5 μ M. In control plates, only DMSO was supplied to leaves or primary root tips at a final concentration of 0.1% (v/v).

Root Growth Measurements

After 15 d of incubation on SAPs, root systems were scanned by an Epson Expression 1000XL scanner at a resolution of 300 dpi. Root growth measurements were taken from scanned images using WhinRHIZO version Pro2007d software (Regents Instruments Canada). Lateral root primordia were counted using conventional light microscopy (Olympus BH). Since high homogenous Fe supplies resulted in a slight reduction in primary root length (Figure 1A), lateral root numbers were expressed as lateral root density (Dubrovsky et al., 2009). Developmental stages of lateral root initials were classified according to Malamy and Benfey (1997). All the experiments were performed at least twice and yielded similar results.

Histochemical Analysis

Seven-day-old *Arabidopsis ProCYCB1;1:GUS* (*cycb1:uid*; Ferreira et al., 1994) or *DR5-GUS* (Ulmasov et al., 1997) lines were germinated in half-strength MS Fe-free media and transferred to separated agar plates with the primary root apex touching the middle segment. Just before the primary root left the middle segment (3 d of treatments) and after growth resulted in contact with the third segment (6 d of treatments), root systems from the middle segment were excised and stained for GUS activity. For the staining, root samples were incubated overnight at 37°C in a GUS reaction buffer containing 0.4 mg mL⁻¹ of 5-bromo-4-chloro-3-indolyl- β -D-glucuronide, 50 mM sodium phosphate, pH 7.2, and 0.5 mM ferrocyanide. After 12 h, the roots were cleared and mounted as described by Malamy and Benfey (1997). For each treatment, 30 to 40 roots were analyzed. Before plants were transferred to treatments, a GUS staining analysis of roots growing in the upper segment revealed that 1.0 \pm 0.01 lateral roots were at the preemerged stage and 1.43 \pm 0.53 had already emerged.

Microscopy Analyses

Lateral root meristem and epidermal cell lengths were measured on micrographs of lateral roots from at least 14 seedlings taken by a Zeiss microscope (Axiovert 200M) equipped with an AxioCam HR camera. Meristem length was assessed as the distance between the quiescent center and the first elongating cell and was measured with AxioVision40 version 4.8.1.0 software (Zeiss). The same software was also used to determine the length of epidermal cells. YFP and GFP images were obtained with an LSM 510 META confocal microscope (Zeiss). Excitation light produced by an argon laser was adjusted to 488 nm and emission filters of 510 to 525 nm and 505 to 530 nm allowed the detection of GFP and YFP fluorescence signals, respectively. Image superimposition and fluorescence quantification were made by means of the Zeiss LSM 510 software version 3.0. The same microscope settings were used to record all of the confocal sections across samples.

Mineral Element and Chlorophyll Analysis

Shoots of agar-grown plants were briefly rinsed with double-distilled water and dried at 80°C. Samples consisting of ~20 shoots were digested with HNO₃ in polytetrafluoroethylene vials in a pressurized microwave digestion system (UltraCLAVE IV; MLS GmbH). Elemental analysis was performed by inductively coupled plasma mass spectrometry (ELAN 6000; Perkin-Elmer Sciex). The certified reference material Standard Reference Material 1575a (pine needles; National Institute of Standards and Technology) was used for quality control, and the recovery rate was >95%. Chlorophyll concentrations were determined by incubating shoot samples with spectrophotometric grade *N,N'*-dimethyl formamide (Sigma-Aldrich) at 4°C for 48 h. The absorbance at 647 and 664 nm was then measured in extracts according to Porra et al. (1989).

Accession Numbers

Sequence data from this article can be found in the Arabidopsis Genome Initiative or GenBank/EMBL databases under the following accession numbers: At5g20730 (ARF7), At1g19220 (ARF19), At2g38120 (AUX1), At2g28160 (FIT), At3g08040 (FRD3), and At4g19690 (IRT1).

Supplemental Data

The following materials are available in the online version of this article.

Supplemental Figure 1. Influence of Fe Deficiency on Root Architecture in *Arabidopsis* Plants.

Supplemental Figure 2. Effect of Homogeneous and Localized Fe Supplies on Lateral Root Development of *Arabidopsis* Plants.

Supplemental Figure 3. Effect of Leaf Fe Supplementation on Lateral Root Growth across the Three Split-Agar Plate Segments.

Supplemental Figure 4. *IRT1* Expression and Histochemical Localization of Fe(III) in Wild-Type and *frd3-1* Roots.

Supplemental Figure 5. Lateral Root Development in Wild-Type and *man1-1* (*frd3-3*) Plants in Response to Localized Fe Supply.

Supplemental Figure 6. Effect of Homogeneous or Localized Fe on the Expression of *IRT1*.

Supplemental Figure 7. Fe Supply to Fe-Deficient Roots Reduces Lateral Root Length in the Middle Segment.

Supplemental Figure 8. Auxin Accumulation in Lateral Roots of Wild-Type and *irt1* Plants in Response to the Supply of High Fe Levels.

Supplemental Figure 9. Lateral Root Elongation in a Set of Auxin Mutants in Response to Localized Fe Availability.

Supplemental Figure 10. Physiological Characterization of *aux1-T* under Homogeneous and Localized Supply of Fe.

Supplemental References 1. References for Supplemental Figures 4 and 10.

ACKNOWLEDGMENTS

We thank Anderson R. Meda (University of Hohenheim) for technical advice and stimulating discussions. This work was supported by research grants from the Deutsche Forschungsgemeinschaft to N.v.W. (WI1728/6-3 and 13-1) and by a Coordenação de Aperfeiçoamento de Pessoal de Nível Superior/Brasília-Brazil PhD Fellowship to R.F.H.G. We are grateful for *ProCYCB1;1:GUS* seeds from Klaus Harter (Center for Plant Molecular Biology Tübingen, Germany), *Pro35S:FIT, fit-3*, and *irt1-1* seeds (Col-0 background) from Petra Bauer (University of Saarbrücken, Germany), and *ProAUX1:AUX1:YFP* seeds from Jiri Friml (Ghent University, Belgium). The *frd3-1*, *man1-1* (*frd3-3*), *nit1-3*, and *axr1-3* mutant lines were obtained from the ABRC, Nottingham; and *aux1-T*, *tir1-T*, and *pin2-T* were obtained from the SALK Institute.

AUTHOR CONTRIBUTIONS

R.F.H.G., J.E.L., and N.v.W. designed the experiments. R.F.H.G. and J.E.L. performed the experiments. R.F.H.G. and N.v.W. wrote the article.

Received October 24, 2011; revised November 15, 2011; accepted December 9, 2011; published January 10, 2012.

REFERENCES

- Bao, J., Chen, F.J., Gu, R.L., Wang, G.Y., Zhang, F.S., and Mi, G.H. (2007). Lateral root development of two *Arabidopsis* auxin transport mutants, *aux1-7* and *eir1-1*, in response to nitrate supplies. *Plant Sci.* **173**: 417–425.
- Bauer, P., Ling, H.Q., and Gueriot, M.L. (2007). FIT, the FER-LIKE IRON DEFICIENCY INDUCED TRANSCRIPTION FACTOR in *Arabidopsis*. *Plant Physiol. Biochem.* **45**: 260–261.
- Casimiro, I., Beeckman, T., Graham, N., Bhalerao, R., Zhang, H., Casero, P., Sandberg, G., and Bennett, M.J. (2003). Dissecting *Arabidopsis* lateral root development. *Trends Plant Sci.* **8**: 165–171.
- Casimiro, I., Marchant, A., Bhalerao, R.P., Beeckman, T., Dhooge, S., Swarup, R., Graham, N., Inzé, D., Sandberg, G., Casero, P.J., and Bennett, M. (2001). Auxin transport promotes *Arabidopsis* lateral root initiation. *Plant Cell* **13**: 843–852.
- Chaney, R.L. (1988). Plants can utilize iron from Fe-N,N'-Di-(2-hydroxybenzoyl)-ethylenediamine-N,N'-diacetic acid, a ferric chelate with 106 greater formation constant than Fe-Eddha. *J. Plant Nutr.* **11**: 1033–1050.
- Chen, W.W., Yang, J.L., Qin, C., Jin, C.W., Mo, J.H., Ye, T., and Zheng, S.J. (2010). Nitric oxide acts downstream of auxin to trigger root ferric-chelate reductase activity in response to iron deficiency in *Arabidopsis*. *Plant Physiol.* **154**: 810–819.
- Colangelo, E.P., and Gueriot, M.L. (2004). The essential basic helix-loop-helix protein FIT1 is required for the iron deficiency response. *Plant Cell* **16**: 3400–3412.
- Delhaize, E. (1996). A metal-accumulator mutant of *Arabidopsis thaliana*. *Plant Physiol.* **111**: 849–855.
- De Smet, I., et al. (2007). Auxin-dependent regulation of lateral root positioning in the basal meristem of *Arabidopsis*. *Development* **134**: 681–690.

- Drew, M.C.** (1975). Comparison of effects of a localized supply of phosphate, nitrate, ammonium and potassium on growth of seminal root system, and shoot, in barley. *New Phytol.* **75**: 479–490.
- Dubrovsky, J.G., Rost, T.L., Colón-Carmona, A., and Doerner, P.** (2001). Early primordium morphogenesis during lateral root initiation in *Arabidopsis thaliana*. *Planta* **214**: 30–36.
- Dubrovsky, J.G., Soukup, A., Napsucially-Mendivil, S., Jeknic, Z., and Ivanchenko, M.G.** (2009). The lateral root initiation index: an integrative measure of primordium formation. *Ann. Bot. (Lond.)* **103**: 807–817.
- Durrett, T.P., Gassmann, W., and Rogers, E.E.** (2007). The FRD3-mediated efflux of citrate into the root vasculature is necessary for efficient iron translocation. *Plant Physiol.* **144**: 197–205.
- Enomoto, Y., Hodoshima, H., Shimada, H., Shoji, K., Yoshihara, T., and Goto, F.** (2007). Long-distance signals positively regulate the expression of iron uptake genes in tobacco roots. *Planta* **227**: 81–89.
- Ferreira, P.C.G., Hemerly, A.S., Engler, J.D., van Montagu, M., Engler, G., and Inzé, D.** (1994). Developmental expression of the *Arabidopsis* cyclin gene *cyc1At*. *Plant Cell* **6**: 1763–1774.
- Fischer, U., Ikeda, Y., Ljung, K., Serralbo, O., Singh, M., Heidstra, R., Palme, K., Scheres, B., and Grebe, M.** (2006). Vectorial information for *Arabidopsis* planar polarity is mediated by combined AUX1, EIN2, and GNOM activity. *Curr. Biol.* **16**: 2143–2149.
- Friml, J., Vieten, A., Sauer, M., Weijers, D., Schwarz, H., Hamann, T., Offringa, R., and Jürgens, G.** (2003). Efflux-dependent auxin gradients establish the apical-basal axis of *Arabidopsis*. *Nature* **426**: 147–153.
- Fukaki, H., Okushima, Y., and Tasaka, M.** (2007). Auxin-mediated lateral root formation in higher plants. *Int. Rev. Cytol.* **256**: 111–137.
- Fukaki, H., Tameda, S., Masuda, H., and Tasaka, M.** (2002). Lateral root formation is blocked by a gain-of-function mutation in the SOLITARY-ROOT/IAA14 gene of *Arabidopsis*. *Plant J.* **29**: 153–168.
- Fukaki, H., and Tasaka, M.** (2009). Hormone interactions during lateral root formation. *Plant Mol. Biol.* **69**: 437–449.
- Geldner, N., Richter, S., Vieten, A., Marquardt, S., Torres-Ruiz, R.A., Mayer, U., and Jürgens, G.** (2004). Partial loss-of-function alleles reveal a role for GNOM in auxin transport-related, post-embryonic development of *Arabidopsis*. *Development* **131**: 389–400.
- Giehl, R.F.H., Meda, A.R., and von Wirén, N.** (2009). Moving up, down, and everywhere: Signaling of micronutrients in plants. *Curr. Opin. Plant Biol.* **12**: 320–327.
- Green, L.S., and Rogers, E.E.** (2004). FRD3 controls iron localization in *Arabidopsis*. *Plant Physiol.* **136**: 2523–2531.
- Grusak, M.A., and Pezeshgi, S.** (1996). Shoot-to-root signal transmission regulates root Fe(III) reductase activity in the *dgl* mutant of pea. *Plant Physiol.* **110**: 329–334.
- Hinsinger, P., Gobran, G.R., Gregory, P.J., and Wenzel, W.W.** (2005). Rhizosphere geometry and heterogeneity arising from root-mediated physical and chemical processes. *New Phytol.* **168**: 293–303.
- Hodge, A.** (2006). Plastic plants and patchy soils. *J. Exp. Bot.* **57**: 401–411.
- Jain, A., Poling, M.D., Smith, A.P., Nagarajan, V.K., Lahner, B., Meagher, R.B., and Raghothama, K.G.** (2009). Variations in the composition of gelling agents affect morphophysiological and molecular responses to deficiencies of phosphate and other nutrients. *Plant Physiol.* **150**: 1033–1049.
- Jakoby, M., Wang, H.Y., Reidt, W., Weisshaar, B., and Bauer, P.** (2004). FRU (BHLH029) is required for induction of iron mobilization genes in *Arabidopsis thaliana*. *FEBS Lett.* **577**: 528–534.
- Kim, S.A., and Guerinot, M.L.** (2007). Mining iron: Iron uptake and transport in plants. *FEBS Lett.* **581**: 2273–2280.
- Krouk, G., et al.** (2010). Nitrate-regulated auxin transport by NRT1.1 defines a mechanism for nutrient sensing in plants. *Dev. Cell* **18**: 927–937.
- Landsberg, E.C.** (1986). Function of rhizodermal transfer cells in the stress response mechanism of *Capsicum annuum* L. *Plant Physiol.* **82**: 511–517.
- Laskowski, M., Biller, S., Stanley, K., Kajstura, T., and Prusty, R.** (2006). Expression profiling of auxin-treated *Arabidopsis* roots: Toward a molecular analysis of lateral root emergence. *Plant Cell Physiol.* **47**: 788–792.
- Laskowski, M., Grieneisen, V.A., Hofhuis, H., Hove, C.A., Hogeweg, P., Marée, A.F.M., and Scheres, B.** (2008). Root system architecture from coupling cell shape to auxin transport. *PLoS Biol.* **6**: e307.
- Lewis, D.R., Miller, N.D., Splitt, B.L., Wu, G.S., and Spalding, E.P.** (2007). Separating the roles of acropetal and basipetal auxin transport on gravitropism with mutations in two *Arabidopsis* multidrug resistance-like ABC transporter genes. *Plant Cell* **19**: 1838–1850.
- Lewis, D.R., Ramirez, M.V., Miller, N.D., Vallabhaneni, P., Ray, W.K., Helm, R.F., Winkel, B.S.J., and Muday, G.K.** (2011). Auxin and ethylene induce flavonol accumulation through distinct transcriptional networks. *Plant Physiol.* **156**: 144–164.
- Lima, J.E., Kojima, S., Takahashi, H., and von Wirén, N.** (2010). Ammonium triggers lateral root branching in *Arabidopsis* in an AMMONIUM TRANSPORTER1;3-dependent manner. *Plant Cell* **22**: 3621–3633.
- Lincoln, C., Britton, J.H., and Estelle, M.** (1990). Growth and development of the *axr1* mutants of *Arabidopsis*. *Plant Cell* **2**: 1071–1080.
- Ling, H.Q., Bauer, P., Berczky, Z., Keller, B., and Ganai, M.** (2002). The tomato *fer* gene encoding a bHLH protein controls iron-uptake responses in roots. *Proc. Natl. Acad. Sci. USA* **99**: 13938–13943.
- Linkohr, B.I., Williamson, L.C., Fitter, A.H., and Leyser, H.M.O.** (2002). Nitrate and phosphate availability and distribution have different effects on root system architecture of *Arabidopsis*. *Plant J.* **29**: 751–760.
- López-Bucio, J., Cruz-Ramírez, A., and Herrera-Estrella, L.** (2003). The role of nutrient availability in regulating root architecture. *Curr. Opin. Plant Biol.* **6**: 280–287.
- Lucena, C., Waters, B.M., Romera, F.J., García, M.J., Morales, M., Alcántara, E., and Pérez-Vicente, R.** (2006). Ethylene could influence ferric reductase, iron transporter, and H⁺-ATPase gene expression by affecting *FER* (or *FER*-like) gene activity. *J. Exp. Bot.* **57**: 4145–4154.
- Malamy, J.E., and Benfey, P.N.** (1997). Organization and cell differentiation in lateral roots of *Arabidopsis thaliana*. *Development* **124**: 33–44.
- Marchant, A., Bhalerao, R., Casimiro, I., Eklöf, J., Casero, P.J., Bennett, M., and Sandberg, G.** (2002). AUX1 promotes lateral root formation by facilitating indole-3-acetic acid distribution between sink and source tissues in the *Arabidopsis* seedling. *Plant Cell* **14**: 589–597.
- Marschner, H.** (1995). *Mineral Nutrition of Higher Plants*. (London: Academic Press).
- Men, S.Z., Boutté, Y., Ikeda, Y., Li, X.G., Palme, K., Stierhof, Y.D., Hartmann, M.A., Moritz, T., and Grebe, M.** (2008). Sterol-dependent endocytosis mediates post-cytokinetic acquisition of PIN2 auxin efflux carrier polarity. *Nat. Cell Biol.* **10**: 237–244.
- Morales, F., Abadía, A., and Abadía, J.** (1990). Characterization of the xanthophyll cycle and other photosynthetic pigment changes induced by iron-deficiency in sugar-beet (*Beta vulgaris* L). *Plant Physiol.* **94**: 607–613.
- Müller, M., and Schmidt, W.** (2004). Environmentally induced plasticity of root hair development in *Arabidopsis*. *Plant Physiol.* **134**: 409–419.
- Murashige, T., and Skoog, F.** (1962). A revised medium for rapid growth and bio assays with tobacco tissue cultures. *Physiol. Plant.* **15**: 473–497.
- Normanly, J., Grisafi, P., Fink, G.R., and Bartel, B.** (1997). *Arabidopsis*

- mutants resistant to the auxin effects of indole-3-acetonitrile are defective in the nitrilase encoded by the *NIT1* gene. *Plant Cell* **9**: 1781–1790.
- Okushima, Y., Fukaki, H., Onoda, M., Theologis, A., and Tasaka, M.** (2007). ARF7 and ARF19 regulate lateral root formation via direct activation of LBD/ASL genes in *Arabidopsis*. *Plant Cell* **19**: 118–130.
- Péret, B., De Rybel, B., Casimiro, I., Benková, E., Swarup, R., Laplaze, L., Beeckman, T., and Bennett, M.J.** (2009). *Arabidopsis* lateral root development: An emerging story. *Trends Plant Sci.* **14**: 399–408.
- Pérez-Torres, C.A., López-Bucio, J., Cruz-Ramírez, A., Ibarra-Laclette, E., Dharmasiri, S., Estelle, M., and Herrera-Estrella, L.** (2008). Phosphate availability alters lateral root development in *Arabidopsis* by modulating auxin sensitivity via a mechanism involving the TIR1 auxin receptor. *Plant Cell* **20**: 3258–3272.
- Perry, P., Linke, B., and Schmidt, W.** (2007). Reprogramming of root epidermal cells in response to nutrient deficiency. *Biochem. Soc. Trans.* **35**: 161–163.
- Porra, R.J., Thompson, W.A., and Kriedemann, P.E.** (1989). Determination of accurate extinction coefficients and simultaneous equations for assaying chlorophyll-A and chlorophyll-B extracted with 4 different solvents: Verification of the concentration of chlorophyll standards by atomic-absorption spectroscopy. *Biochim. Biophys. Acta* **975**: 384–394.
- Remans, T., Nacry, P., Pervent, M., Filleur, S., Diatloff, E., Mounier, E., Tillard, P., Forde, B.G., and Gojon, A.** (2006). The *Arabidopsis* NRT1.1 transporter participates in the signaling pathway triggering root colonization of nitrate-rich patches. *Proc. Natl. Acad. Sci. USA* **103**: 19206–19211.
- Rogers, E.E., and Guerinot, M.L.** (2002). FRD3, a member of the multidrug and toxin efflux family, controls iron deficiency responses in *Arabidopsis*. *Plant Cell* **14**: 1787–1799.
- Römheld, V., and Marschner, H.** (1981). Effect of Fe stress on utilization of Fe chelates by efficient and inefficient plant-species. *J. Plant Nutr.* **3**: 551–560.
- Sabatini, S., Beis, D., Wolkenfelt, H., Murfett, J., Guilfoyle, T., Malamy, J., Benfey, P., Leyser, O., Bechtold, N., Weisbeek, P., and Scheres, B.** (1999). An auxin-dependent distal organizer of pattern and polarity in the *Arabidopsis* root. *Cell* **99**: 463–472.
- Schmidt, W., and Schikora, A.** (2001). Different pathways are involved in phosphate and iron stress-induced alterations of root epidermal cell development. *Plant Physiol.* **125**: 2078–2084.
- Schmidt, W., Tittel, J., and Schikora, A.** (2000). Role of hormones in the induction of iron deficiency responses in *Arabidopsis* roots. *Plant Physiol.* **122**: 1109–1118.
- Swarup, K., et al.** (2008). The auxin influx carrier LAX3 promotes lateral root emergence. *Nat. Cell Biol.* **10**: 946–954.
- Swarup, R., Friml, J., Marchant, A., Ljung, K., Sandberg, G., Palme, K., and Bennett, M.** (2001). Localization of the auxin permease AUX1 suggests two functionally distinct hormone transport pathways operate in the *Arabidopsis* root apex. *Genes Dev.* **15**: 2648–2653.
- Swarup, R., et al.** (2004). Structure-function analysis of the presumptive *Arabidopsis* auxin permease AUX1. *Plant Cell* **16**: 3069–3083.
- Swarup, R., Kramer, E.M., Perry, P., Knox, K., Leyser, H.M., Haseloff, J., Beemster, G.T., Bhalerao, R., and Bennett, M.J.** (2005). Root gravitropism requires lateral root cap and epidermal cells for transport and response to a mobile auxin signal. *Nat. Cell Biol.* **7**: 1057–1065.
- Ulmasov, T., Murfett, J., Hagen, G., and Guilfoyle, T.J.** (1997). Aux/IAA proteins repress expression of reporter genes containing natural and highly active synthetic auxin response elements. *Plant Cell* **9**: 1963–1971.
- Varotto, C., Maiwald, D., Pesaresi, P., Jahns, P., Salamini, F., and Leister, D.** (2002). The metal ion transporter IRT1 is necessary for iron homeostasis and efficient photosynthesis in *Arabidopsis thaliana*. *Plant J.* **31**: 589–599.
- Vert, G., Grotz, N., Dédaldéchamp, F., Gaymard, F., Guerinot, M.L., Briat, J.F., and Curie, C.** (2002). IRT1, an *Arabidopsis* transporter essential for iron uptake from the soil and for plant growth. *Plant Cell* **14**: 1223–1233.
- Vert, G.A., Briat, J.F., and Curie, C.** (2003). Dual regulation of the *Arabidopsis* high-affinity root iron uptake system by local and long-distance signals. *Plant Physiol.* **132**: 796–804.
- Wu, G., Lewis, D.R., and Spalding, E.P.** (2007). Mutations in *Arabidopsis* multidrug resistance-like ABC transporters separate the roles of acropetal and basipetal auxin transport in lateral root development. *Plant Cell* **19**: 1826–1837.
- Zhang, H., Jennings, A., Barlow, P.W., and Forde, B.G.** (1999). Dual pathways for regulation of root branching by nitrate. *Proc. Natl. Acad. Sci. USA* **96**: 6529–6534.
- Zhang, H.M., and Forde, B.G.** (1998). An *Arabidopsis* MADS box gene that controls nutrient-induced changes in root architecture. *Science* **279**: 407–409.